Structural Effect of Adding Paired and Unpaired Electrons to Otherwise Identical Transition Metal Systems. Relation between the Magnetic and Structural Properties in Iron(III) Complexes, Observation of a New Intermediate Iron(III) Spin ($S = \frac{3}{2}$) State, and Structures of Benzene Solvated Tris(4-morpholinecarbodithioato-*S,S'*)chromium(III), -iron(III), -cobalt(III), -rhodium(III), and -iridium(III)

Ray J. Butcher and Ekk Sinn*

Contribution from the Chemistry Department, University of Virginia, Charlottesville, Virginia 22901. *Received September 2, 1975*

Abstract: The crystal and molecular structures of the title complexes were solved by single-crystal x-ray diffraction using computer techniques. Crystal data: $Cr(S_2CNC_4H_8O)_3\cdot(C_6H_6)_2$, $C2/c$, $Z = 4$, $a = 19.314$ (5) Å, $b = 18.046$ (4) Å, $c = 12.307$ (2) Å, $\beta = 53.48$ (2)°, $U = 3448$ Å^3, $R = 3.2\%$, 1674 reflections; $Fe(S_2CNC_4H_8O)_3\cdot(C_6H_6)_2$, $C2/c$, $Z = 4$, $a = 19.22$ (1) Å, $b = 17.916$ (4) Å, $c = 12.275$ (4) Å, $\beta = 53.41$ (3)°, $U = 3394$ Å^3, $R = 4.7\%$, 3026 reflections; $Co(S_2CNC_4H_8O)_3\cdot(C_6H_6)_2$, $C2/c$, $Z = 4$, $a = 19.094$ (3) Å, $b = 17.874$ (2) Å, $c = 12.283$ (2) Å, $\beta = 53.15$ (1)°, $U = 3354$ Å^3, $R = 3.6\%$, 2378 reflections; $Rh(S_2CNC_4H_8O)_3\cdot(C_6H_6)_2$, $C2/c$, $Z = 4$, $a = 19.327$ (6) Å, $b = 18.036$ (5) Å, $c = 12.286$ (5) Å, $\beta = 52.43$ (6)°, $U = 3395$ Å^3, $R = 5.4\%$, 1875 reflections; $Ir(S_2CNC_4H_8O)_3\cdot(C_6H_6)_2$, $C2/c$, $Z = 4$, $a = 19.390$ (9) Å, $b = 18.108$ (8) Å, c 12.256 (9) Å, $\beta = 52.09$ (5)°, $U = 3395$ Å^3, $R = 5.0\%$, 1961 reflections. The complex molecules are reasonably well separated from one another and from the solvating benzene molecules. In each case the metal atom and one ligand atom lie along a twofold axis. The average metal–ligand bond length, ⟨M–L⟩, increases as the number of unpaired d electrons increases, especially in the t_2 subshell: ⟨Co–S⟩ = 2.273 (1) Å (t_2^6), ⟨Fe–S⟩ = 2.317 (1) Å (mainly t_2^5, some $t_2^3e^2$), ⟨Cr–S⟩ = 2.396 (3) Å (t_2^3). ⟨M–L⟩ increases vertically downwards from the first to the second or third transition series: 2.273 (1) in $3d^6$, 2.365 (4) and 2.372 (3) Å in $4d^6$ and $5d^6$. The temperature dependence of the magnetic moment of the ferric complex differs dramatically from that of the analogous complex solvated by dichloromthane and that of the unsolvated complex, though each of the three forms exhibits a spin state equilibrium. This equilibrium is displaced towards the low and high spin sides in the C_6H_6 solvate and the unsolvated complexes, respectively. However, in the dichloromethane solvate, the equilibrium is between a new intermediate quartet ($S = \frac{3}{2}$) state and the high spin ($S = \frac{5}{2}$) state, and this difference in the magnetic properties is reflected in an ⟨M–L⟩ difference of more than 0.1 Å between the benzene and dichloromethane solvated complexes. An even greater ⟨M–L⟩ difference is therefore implied for a transition from pure low spin to pure high spin species. The M–L stretching frequencies are compatible with but inconclusive about a spin-state equilibrium in the iron complexes rather than a single mixed spin state.

A wide range of ferric complexes with ligands of the dithiocarbamate type exhibits a $^6A_1$–$^2T_2$ spin state equilibrium.[1] Rather than a simple Tanabe-Sugano type crossing between high and low spins, such equilibria are considered to involve distinct species having different metal–ligand bond lengths and therefore different ligand field strengths. The low spin form has fewer occupied orbitals and hence the smaller volume, the volume reduction being concentrated mainly in the metal–ligand sphere.[2,4] The equilibrium is very sensitive to such factors as temperature and pressure. Moreover, the large differences that exist between magnetic properties in the solid diethyl, di-*n*-propyl, and di-*n*-butyl complexes in the solid compared to solutions suggest that packing effects in the solid crystalline lattice are also important.[1] Interest in solvates of tris(dithiocarbamate) complexes also stems from the observation of solvent effects in many dithiocarbamate NMR spectra.[5]

Tris(4-morpholinecarbodithioato-*S,S'*)iron(III) solvates with one molecule of dichloromethane[6] and with two molecules of benzene (FeMBz) are obtainable as good single crystals, and their magnetic properties differ. These compounds therefore present an ideal opportunity to determine how much difference lattice forces can make, and to examine the detailed geometry of the same complex under different conditions, without the need to resort to extreme conditions of pressure or temperature.

The benzene solvated analogues of FeMBz with Cr, Mn, Co, Rh, and Ir also form and, of these, all but MnMBz could be obtained as crystals large enough for crystal structure determination. These provide further information on the effect of altering the number of d electrons in a "standard" complex, keeping the ligand and the included solvent molecules constant and the lattice effects almost constant.[7,8]

Experimental Section

The dichloromethane solvates $M(S_2CNC_4H_8O)_3\cdot CH_2Cl_2$ were prepared as previously described.[6,7] The dibenzene solvates were obtained by slow evaporation of benzene solutions to which ethanol had been added slowly to the point of incipient precipitate. Due to the low solubility of the complexes in benzene, the crystals formed by this method tend to be fairly small. The manganese complex decomposed rapidly in solution, leading to small yields and crystals too small for x-ray data collection.

Crystal Data for CrMBz. $CrS_6O_3N_3C_{27}H_{36}$; M = 695; space group $C2/c$; $Z = 4$; $a = 19.314$ (5), $b = 18.046$ (4), $c = 12.307$ (2) Å; $\beta = 53.48$ (2)°; $U = 3448$ Å^3; μ(Mo Kα) = 7.3 cm^{-1}, $d_c = 1.34$, $d_o = 1.29$ (3) g cm^{-3}; $F(000) = 1452$.

Crystal Data for FeMBz. $FeS_6O_3N_3C_{27}H_{36}$; M = 699; space group $C2/c$; $Z = 4$; $a = 19.22$ (1), $b = 17.916$ (4), $c = 12.275$ (4) Å; $\beta = 53.41$ (3)°; $U = 3394$ Å^3; μ(Mo Kα) = 8.5 cm^{-1}; $d_c = 1.38$, $d_o = 1.36$ (3) g cm^{-3}; $F(000) = 1460$.

Crystal Data for CoMBz. $CoS_6O_3N_3C_{27}H_{36}$; M = 702; space group $C2/c$; $Z = 4$; $a = 19.094$ (3), $b = 17.874$ (2), $c = 12.283$

(2) Å; β = 53.15 (1)°; U = 3354 Å^3, μ(Mo Kα) = 9.2 cm^{-1}; d_c = 1.39, d_o = 1.40 (3) g cm^{-3}; F(000) = 1464.

Crystal Data for RhMBz. $RhS_6O_3N_3C_{27}H_{36}$; M = 746; space group $C2/c$; Z = 4; a = 19.327 (6), b = 18.036 (5), c = 12.286 (5) Å; β = 52.43 (6)°; U = 3395 Å^3, μ(Mo Kα) = 8.8 cm^{-1}; d_c = 1.46, d_o = 1.54 (3) g cm^{-3}, F(000) = 1536.

Crystal Data for IrMBz. $IrS_6O_3N_3C_{27}H_{36}$; M = 835; space group $C2/c$; Z = 4; a = 19.390 (9), b = 18.108 (8), c = 12.256 (9) Å; β = 52.09 (5)°; U = 3395 Å^3, μ(Mo Kα) = 45.4 cm^{-1}; d_c = 1.63, d_o = 1.62 (3) g cm^{-3}; F(000) = 1664.

Crystal Data for MnMBz (from precession photographs): space group $C2/c$; a = 19.2, b = 17.9, c = 12.4 Å; β = 53.3°.

For each crystal, except MnMBz, the Enraf-Nonius program SEARCH was used to obtain 15 accurately centered reflections which were then used in the program INDEX to obtain an orientation matrix for data collection and also approximate cell dimensions. Refined cell dimensions and their estimated standard deviations were obtained from least-squares refinement of 28 accurately centered reflections. The mosaicity of each crystal was examined by the ω scan technique and judged to be satisfactory. It is apparent from the crystal data that the six complexes are at least approximately isomorphous, which is useful not only for the comparative study contemplated but also in the solution of the structures.

Collection and Reduction of the Data. Diffraction data were collected at 292 K on an Enraf-Nonius four-circle CAD-4 diffractometer controlled by a PDP8/M computer, using Mo Kα radiation from a highly oriented graphite crystal monochromator. The θ–2θ scan technique was used to record the intensities for all reflections for which 1° < 2θ < 52° for CrMBz, FeMBz, and CoMBz and 1° < 2θ < 47° for RhMBz and IrMBz. Scan widths (SW) were calculated from the formula SW = $A + B \tan\theta$ where A is estimated from the mosaicity of the crystal and B allows for the increase in width of peak due to Kα_1 and Kα_2 splitting. The values of A and B were 0.6° and 0.2°, respectively. This calculated scan angle is extended at each side by 25% for background determination (BG1 and BG2). The net count (NC) is then calculated as NC = TOT − 2(BG1 + BG2) where TOT is the estimated peak intensity. Reflection data were considered insignificant if intensities registered less then ten counts above background on a rapid prescan, such reflections being rejected automatically by the computer.

The intensities of four standard reflections, monitored for each crystal at 100 reflection intervals, showed no greater fluctuations during the data collection than those expected from Poisson statistics. The raw intensity data were corrected for Lorentz-polarization effects and then for absorption, spherical absorption corrections being applied to FeMBz and RhMBz due to the absence of sufficiently well-defined crystal faces; no absorption correction was applied for CrMBz. The absence of absorption corrections on this small crystal should have at most a small effect on the temperature factors (μ = 7.3 cm^{-1}). After averaging the intensities of equivalent reflections, the data were reduced to 3504, 3259, 3178, 2113, and 2100 independent intensities for CrMBz, FeMBz, CoMBz, RhMBz, and IrMBz respectively, of which 1674, 3026, and 2378 had $F_o^2 > 3\sigma(F_o^2)$ for CrMBz, FeMBz, and CoMBz, respectively, and 1875 had $F_o^2 > 2\sigma(F_o^2)$ for RhMBz and 1961 had $F_o^2 > \sigma(F_o^2)$ for IrMBz, where $\sigma(F_o^2)$ was estimated from counting statistics.[9] These data were used in the final refinement of the structural parameters.

Refinement of the Structure. Full-matrix least-squares refinement was based on F, and the function minimized was $\Sigma w(|F_o| - |F_d|)^2$. The weights w were taken as $[2F_o/\sigma(F_o^2)]^2$ where $|F_d|$ and $|F_d|$ are the observed and calculated structure factor amplitudes. The atomic scattering factors for non-hydrogen atoms were taken from Cromer and Waber[10] and those for hydrogen from Stewart.[11] The effects of anomalous dispersion were included in F_c using Cromer's values[12] for $\Delta f'$ and $\Delta f''$. Agreement factors are defined as $R = \Sigma||F_o| - |F_d||/\Sigma|F_o|$ and $R_w = (\Sigma w(|F_o| - |F_d|)^2/\Sigma w|F_o|^2)^{1/2}$.

Examination of a three-dimensional Patterson function calculated from all data for IrMBz, and the unit cell volume, suggested that the asymmetric unit contains only half of a complex molecule, with the metal atom on a twofold axis 0, 0.19, 0.25. After full-matrix least-squares refinement, this model converged with R = 25%. A Fourier difference map revealed the three independent sulfur atoms and insertion of these positions produced R = 16% on further refinement.

Since the iridium atom dominates the scattering of IrMBz, the calculation was pursued on the intensity data collected for CoMBz. The metal and sulfur positions were inserted at the positions calculated for IrMBz and refined, R = 39%. The remaining non-hydrogen atoms were located from subsequent Fourier difference maps, with the two methylene atoms of the ligand on the twofold axis showing disorder, R = 11.3%. After refinement, hydrogen atoms were inserted as fixed atoms at the calculated positions, with isotropic temperature factors of 5.0 Å^2, assuming carbon to hydrogen bond lengths of 1.0 Å, and anisotropic temperature factors introduced. After convergence, the hydrogen atoms were inserted at their new calculated positions and refinement of the non-hydrogen atoms continued. The model converged with R = 3.6% and R_w = 4.4%. The positional parameters of non-hydrogen atoms for the other complexes were obtained by refinement of the CrMBz parameters, and the calculation was completed as before. The disorder in the methylene atoms is statistically significant in each case.[13] The models converged with R = 3.2% and R_w = 2.9% for CrMBz, R = 4.7% and R_w = 6.1% for FeMBz, R = 5.4% and R_w = 6.3% for RhMBz, and R = 5.0% and R_w = 5.4% for IrMBz. The error in an observation of unit weight is 0.81, 4.10, 1.53, 1.93, and 1.63 for the Cr, Fe, Co, Rh, and Ir complexes, respectively. A structure factor calculation with all observed and unobserved reflections included (no refinement) gave R = 5.8, 5.1, 4.3, 6.4, and 6.1% for CrMBz, FeMBz, CoMBz, RhMBz, and IrMBz respectively; on this basis, it was decided that careful measurement of reflections rejected automatically during data collection would not significantly improve the results. A final Fourier difference map was featureless. A table of the observed structure factors is available.[14] The computer programs and other computational and technical details are given elsewhere.[15] Densities were determined by flotation in aqueous potassium iodide. Infrared spectra were recorded as Nujol mulls between cesium bromide plates on a Beckman IR-12 filter-grating spectrophotometer. Magnetic susceptibility measurements were made as detailed elsewhere,[16] using a SQUID magnetometer.

Results and Discussion

Final positional and thermal parameters for the complexes CrMBz, FeMBz, CoMBz, RhMBz, and IrMBz are given in Table I. Tables II and III contain the bond lengths and angles. The digits in parentheses in the tables are the estimated standard deviations in the least significant figures quoted and were derived from the inverse matrix in the course of least-squares refinement calculations. Figure 1 is a stereoscopic view of CrMBz and Figure 2 shows the molecular packing in the unit cell. To minimize crowding, the disorder in the ligand ring on the twofold axis is not shown. The other complexes are quite similar and are sufficiently well represented by the same diagram.

From the packing diagram and from the closest intermolecular distances (Table IV), it can be seen that the molecules of the metal complex are well separated from each other and the solvent (Table V). The closest contacts in each case involve the disordered ligand in contact with benzene atoms and with other ligand atoms. The disorder may be the result of displacement of atoms to minimize the nonbonded contacts.

The structures, especially of the MS_6 core, of the complexes CrMBz, FeMBz, CoMBz, RhMBz, and IrMBz can be compared with the dichloromethane solvated analogues, $M(S_2CNC_4H_8O)_3 \cdot CH_2Cl_2$, to obtain direct information on the effects of included solvent molecules and of packing in the lattice. Structure determinations have been carried out on the dichloromethane solvated complexes for M = Cr, Mn, Fe, Co, and Rh.[6,7] Except for the constraint imposed by the crystallographic symmetry on each of the benzene solvated complexes, the main difference between the two groups is in the iron coordination spheres, suggesting different spin-state populations depending on the solvate. For each of the other metals, where both structures are available, the coordination spheres are quite similar independent

Table I. Positional and Thermal Parameters[a] and Their Estimated Standard Deviations

(a) CrMBz

Atom	x	y	z	$\beta_{1,1}$	$\beta_{2,2}$	$\beta_{3,3}$	$\beta_{1,2}$	$\beta_{1,3}$	$\beta_{2,3}$
Cr	0.0000 (0)	0.1937 (1)	0.2500 (0)	0.00510 (7)	0.00387 (8)	0.0110 (2)	0.0000 (0)	−0.0097 (1)	0.0000 (0)
S11	0.0219 (1)	0.0878 (1)	0.1154 (2)	0.00867 (8)	0.00380 (9)	0.0126 (2)	0.0001 (2)	−0.0157 (1)	0.0007 (2)
S12	−0.0036 (1)	0.2813 (1)	0.1061 (2)	0.00530 (8)	0.00421 (9)	0.0128 (2)	−0.0010 (2)	−0.0101 (2)	0.0026 (3)
S22	0.1486 (1)	0.2087 (1)	0.1558 (2)	0.00513 (8)	0.00523 (10)	0.0125 (2)	0.0007 (2)	−0.0097 (2)	−0.0041 (3)
O1	0.0000 (0)	−0.1902 (4)	0.2500 (0)	0.0136 (4)	0.0027 (3)	0.0188 (7)	0.0000 (0)	−0.0232 (6)	0.0000 (0)
O2	0.2682 (3)	0.3226 (3)	0.4010 (4)	0.0085 (2)	0.0073 (3)	0.0254 (5)	0.0023 (4)	−0.0230 (4)	−0.0093 (7)
N1	0.0000 (0)	−0.0356 (5)	0.2500 (0)	0.0234 (6)	0.0042 (5)	0.0204 (8)	0.0000 (0)	−0.0388 (8)	0.0000 (0)
N2	0.1664 (3)	0.2986 (3)	0.3090 (5)	0.0052 (2)	0.0048 (3)	0.0151 (6)	0.0030 (5)	−0.0099 (5)	−0.0075 (8)
C11	0.0000 (0)	0.0374 (5)	0.2500 (0)	0.0092 (4)	0.0026 (5)	0.0169 (10)	0.0000 (0)	−0.0193 (8)	0.0000 (0)
C12A	0.0524 (7)	−0.0847 (8)	0.1121 (11)	0.0053 (6)	0.0065 (8)	0.0155 (14)	0.0010 (12)	−0.0143 (11)	−0.0038 (19)
C12B	−0.0126 (8)	−0.0752 (8)	0.1573 (11)	0.0129 (7)	0.0027 (6)	0.0145 (12)	0.0007 (12)	−0.0229 (11)	−0.0017 (16)
C13A	−0.0109 (7)	−0.1411 (8)	0.1631 (11)	0.0049 (6)	0.0062 (8)	0.0112 (15)	−0.0008 (13)	−0.0077 (13)	−0.0010 (18)
C13B	0.0420 (9)	−0.1487 (7)	0.1234 (12)	0.0117 (8)	0.0026 (6)	0.0097 (15)	0.0022 (13)	−0.0129 (15)	−0.0047 (17)
C21	0.1138 (3)	0.2667 (4)	0.2867 (5)	0.0056 (3)	0.0038 (3)	0.0139 (7)	−0.0011 (5)	−0.0124 (6)	−0.0008 (8)
C22	0.2586 (4)	0.2865 (4)	0.2226 (6)	0.0058 (3)	0.0068 (4)	0.0178 (8)	0.0013 (7)	−0.0130 (6)	−0.0045 (11)
C23	0.2907 (4)	0.2689 (5)	0.3008 (7)	0.0060 (3)	0.0068 (4)	0.0268 (10)	0.0025 (7)	−0.0175 (7)	−0.0050 (12)
C24	0.1781 (4)	0.3306 (5)	0.4887 (6)	0.0082 (4)	0.0084 (5)	0.0186 (8)	0.0030 (7)	−0.0176 (7)	−0.0084 (11)
C25	0.1392 (4)	0.3487 (4)	0.4219 (7)	0.0067 (3)	0.0061 (4)	0.0215 (9)	0.0030 (6)	−0.0151 (7)	−0.0075 (10)
C1	0.3810 (5)	0.0552 (5)	0.1650 (8)	0.0112 (6)	0.0083 (5)	0.0182 (13)	−0.0079 (9)	−0.0046 (12)	0.0001 (14)
C2	0.2987 (6)	0.0554 (5)	0.2203 (9)	0.0214 (6)	0.0056 (5)	0.0426 (15)	0.0123 (10)	−0.0389 (13)	−0.0116 (14)
C3	0.2525 (7)	0.0157 (7)	0.3263 (10)	0.0108 (7)	0.0219 (9)	0.0228 (15)	−0.0062 (13)	0.0002 (15)	−0.0272 (18)
C4	0.2691 (7)	−0.0215 (6)	0.3891 (9)	0.0302 (8)	0.0163 (6)	0.0131 (13)	−0.0367 (10)	−0.0114 (15)	0.0048 (15)
C5	0.3584 (6)	−0.0264 (5)	0.3209 (8)	0.0319 (7)	0.0058 (5)	0.0385 (11)	−0.0091 (10)	−0.0583 (11)	0.0109 (12)
C6	0.4138 (5)	0.0134 (6)	0.2098 (9)	0.0125 (5)	0.0101 (6)	0.0396 (14)	−0.0012 (10)	−0.0283 (10)	−0.0083 (16)

Atom	x	y	z	B (Å)	Atom	x	y	z	B (Å)
H121	0.0553 (11)	−0.0507 (9)	0.0368 (14)	5.0000	H232	0.3541 (6)	0.2561 (7)	0.2433 (9)	5.0000
H122	0.1128 (11)	−0.0924 (9)	0.0759 (14)	5.0000	H241	0.1463 (6)	0.2803 (7)	0.5448 (9)	5.0000
H123	−0.0081 (10)	−0.0636 (13)	0.0807 (15)	5.0000	H242	0.1573 (6)	0.3669 (7)	0.5704 (9)	5.0000
H124	−0.0748 (10)	−0.1145 (13)	0.2134 (15)	5.0000	H251	0.1605 (6)	0.4037 (6)	0.3867 (9)	5.0000
H131	0.0143 (11)	−0.1871 (9)	0.0731 (16)	5.0000	H252	0.0742 (6)	0.3536 (6)	0.4861 (9)	5.0000
H132	−0.0687 (11)	−0.1401 (9)	0.1943 (16)	5.0000	H1	0.4199 (8)	0.0845 (8)	0.0731 (12)	5.0000
H133	0.0964 (11)	−0.1115 (10)	0.1063 (15)	5.0000	H2	0.2669 (9)	0.0959 (8)	0.1899 (14)	5.0000
H134	0.0632 (11)	−0.1651 (10)	0.0391 (15)	5.0000	H3	0.1834 (10)	0.0062 (9)	0.3576 (16)	5.0000
H221	0.2775 (5)	0.2475 (7)	0.1478 (9)	5.0000	H4	0.2282 (8)	−0.0504 (7)	0.4796 (12)	5.0000
H222	0.2937 (5)	0.3341 (7)	0.1654 (9)	5.0000	H5	0.3886 (8)	−0.0568 (8)	0.3559 (12)	5.0000
H231	0.2605 (6)	0.2167 (7)	0.3486 (9)	5.0000	H6	0.4790 (8)	0.0223 (8)	0.1568 (12)	5.0000

(b) Fe

Atom	x	y	z	$\beta_{1,1}$	$\beta_{2,2}$	$\beta_{3,3}$	$\beta_{1,2}$	$\beta_{1,3}$	$\beta_{2,3}$
Fe	0.0000 (0)	0.19391 (3)	0.2500 (0)	0.00411 (1)	0.00288 (1)	0.00901 (3)	0.0000 (0)	−0.00807 (2)	0.00000 (0)
S21	0.02222 (4)	0.09177 (4)	0.11721 (5)	0.00743 (2)	0.00312 (2)	0.01063 (3)	−0.00020 (3)	−0.01342 (3)	0.00042 (5)
S12	−0.00159 (3)	0.27840 (4)	0.10793 (5)	0.00430 (2)	0.00337 (2)	0.01077 (4)	−0.00098 (3)	−0.00822 (4)	0.00229 (5)
S22	0.14529 (4)	0.20926 (4)	0.15466 (5)	0.00414 (2)	0.00453 (2)	0.01053 (4)	0.00090 (3)	−0.00780 (4)	−0.00370 (5)
O1	0.0000 (0)	−0.1893 (1)	0.2500 (0)	0.01203 (14)	0.00286 (9)	0.0178 (2)	0.0000 (0)	−0.0202 (2)	0.00000 (0)
O2	0.2687 (1)	0.3222 (1)	0.3987 (2)	0.00691 (6)	0.00661 (9)	0.0216 (2)	0.0017 (1)	−0.0192 (1)	−0.00712 (2)
N1	0.0000 (0)	−0.0351 (2)	0.2500 (0)	0.02386 (22)	0.00266 (11)	0.0187 (2)	0.0000 (0)	−0.0362 (3)	0.00000 (0)
N2	0.1661 (1)	0.2982 (1)	0.3090 (2)	0.00487 (6)	0.00463 (8)	0.0139 (2)	0.0012 (1)	−0.0113 (1)	−0.00470 (2)

C11	0.0000 (0)	0.0381 (2)	0.2500 (0)	0.01022 (13)	0.00285 (11)	0.0129 (2)	0.0000 (0)	−0.0186 (2)	0.00000 (0)
C12A	0.0500 (3)	−0.0813 (3)	0.1156 (4)	0.00661 (16)	0.00334 (17)	0.0111 (3)	−0.0004 (3)	−0.0121 (3)	−0.00012 (4)
C12B	−0.0155 (3)	−0.0784 (3)	0.1577 (4)	0.00732 (15)	0.00313 (16)	0.0142 (3)	0.0006 (3)	−0.0162 (3)	−0.00113 (4)
C13A	−0.0121 (3)	−0.1455 (3)	0.1627 (5)	0.00703 (18)	0.00401 (19)	0.0146 (4)	−0.0015 (3)	−0.0135 (3)	−0.00131 (5)
C13B	0.0420 (3)	−0.1446 (3)	0.1237 (4)	0.00850 (20)	0.00309 (17)	0.0136 (4)	0.0011 (3)	−0.0148 (4)	−0.00242 (4)
C21	0.1118 (1)	0.2671 (1)	0.2894 (2)	0.00443 (6)	0.00317 (8)	0.0109 (2)	0.0005 (1)	−0.0093 (1)	−0.00097 (2)
C22	0.2604 (2)	0.2870 (2)	0.2179 (3)	0.00489 (8)	0.00554 (12)	0.0152 (2)	0.0005 (2)	−0.0113 (2)	−0.00320 (3)
C23	0.2907 (2)	0.2657 (2)	0.3009 (3)	0.00595 (9)	0.00621 (14)	0.0196 (3)	0.0014 (2)	−0.0152 (2)	−0.00424 (3)
C24	0.1761 (2)	0.3276 (2)	0.4905 (2)	0.00778 (10)	0.00540 (12)	0.0172 (2)	0.0016 (2)	−0.0170 (2)	−0.00570 (3)
C25	0.1378 (2)	0.3505 (2)	0.4208 (2)	0.00653 (8)	0.00439 (10)	0.0177 (2)	0.0017 (2)	−0.0155 (2)	−0.00541 (3)
C1	0.3763 (3)	0.0593 (2)	0.1608 (4)	0.01367 (25)	0.00512 (15)	0.0255 (5)	−0.0048 (3)	−0.0191 (5)	0.00295 (5)
C2	0.2899 (3)	0.0555 (2)	0.2253 (5)	0.01767 (24)	0.00576 (16)	0.0630 (8)	0.0072 (4)	−0.0489 (5)	−0.01776 (6)
C3	0.2437 (4)	0.0111 (3)	0.3341 (6)	0.00969 (33)	0.01210 (30)	0.0365 (9)	−0.0032 (5)	0.0015 (10)	−0.01889 (8)
C4	0.2787 (4)	−0.0263 (3)	0.3810 (4)	0.02163 (34)	0.01134 (20)	0.0179 (5)	−0.0217 (4)	−0.0085 (7)	−0.00032 (5)
C5	0.3662 (3)	−0.0244 (3)	0.3137 (4)	0.02429 (27)	0.00739 (21)	0.0329 (4)	−0.0085 (4)	−0.0438 (4)	0.00327 (5)
C6	0.4124 (3)	0.0194 (2)	0.2035 (4)	0.00999 (19)	0.00791 (19)	0.0220 (5)	−0.0055 (3)	−0.0137 (4)	−0.00077 (5)

Atom	x	y	z	B (A)	Atom	x	y	z	B (A)
H121	0.1073 (4)	−0.0967 (4)	0.0868 (5)	5.0000	H241	0.1603 (2)	0.3646 (3)	0.5624 (3)	5.0000
H122	0.0534 (4)	−0.0531 (4)	0.0420 (5)	5.0000	H242	0.1526 (2)	0.2773 (3)	0.5324 (3)	5.0000
H123	0.0005 (4)	−0.0490 (4)	0.0769 (5)	5.0000	H251	0.1582 (2)	0.4024 (2)	0.3834 (3)	5.0000
H124	−0.0790 (4)	−0.0939 (4)	0.2096 (5)	5.0000	H252	0.0734 (2)	0.3505 (2)	0.4868 (3)	5.0000
H131	0.0063 (5)	−0.1759 (5)	0.0805 (7)	5.0000	H1	0.4100 (4)	0.0928 (3)	0.0787 (6)	5.0000
H132	−0.0712 (5)	−0.1280 (5)	0.2105 (7)	5.0000	H2	0.2566 (4)	0.0827 (3)	0.1984 (7)	5.0000
H133	0.1008 (4)	−0.1267 (4)	0.0947 (6)	5.0000	H3	0.1785 (4)	0.0018 (4)	0.3935 (7)	5.0000
H134	0.0496 (4)	−0.1746 (4)	0.0494 (6)	5.0000	H4	0.2431 (5)	−0.0508 (4)	0.4684 (6)	5.0000
H221	0.2889 (2)	0.3344 (2)	0.1680 (3)	5.0000	H5	0.3939 (4)	−0.0624 (4)	0.3467 (5)	5.0000
H222	0.2743 (2)	0.2465 (2)	0.1513 (3)	5.0000	H6	0.4766 (4)	0.0247 (4)	0.1527 (5)	5.0000
H231	0.3550 (2)	0.2583 (3)	0.2398 (4)	5.0000					
H232	0.2625 (2)	0.2171 (3)	0.3493 (4)	5.0000					

(c) Co

Atom	x	y	z	$\beta_{1,1}$	$\beta_{2,2}$	$\beta_{3,3}$	$\beta_{1,2}$	$\beta_{1,3}$	$\beta_{2,3}$
Co	0.0000 (0)	0.19255 (5)	0.2500 (0)	0.00415 (2)	0.00274 (3)	0.00875 (5)	0.0000 (0)	−0.00793 (4)	0.0000 (0)
S11	0.01957 (7)	0.09273 (7)	0.11988 (9)	0.00724 (4)	0.00297 (4)	0.01053 (7)	−0.00021 (7)	−0.01306 (6)	0.00022 (9)
S21	0.00067 (6)	0.27762 (7)	0.38739 (9)	0.00422 (3)	0.00320 (4)	0.01031 (8)	0.00090 (6)	−0.00807 (7)	−0.00211 (10)
S22	0.14427 (6)	0.20531 (7)	0.15534 (9)	0.00422 (3)	0.00396 (4)	0.01032 (8)	0.00101 (7)	−0.00799 (7)	−0.00315 (10)
O1	0.0000 (0)	−0.1903 (2)	0.2500 (0)	0.0110 (2)	0.0028 (2)	0.0171 (4)	0.0000 (0)	−0.0189 (4)	0.0000 (0)
O2	0.2683 (2)	0.3211 (2)	0.3980 (3)	0.0063 (1)	0.0064 (2)	0.0190 (3)	0.0013 (2)	−0.0166 (2)	−0.0058 (4)
N1	0.0000 (0)	−0.0352 (3)	0.2500 (0)	0.0214 (3)	0.0026 (2)	0.0178 (4)	0.0000 (0)	−0.0335 (4)	0.0000 (0)
N2	0.1663 (2)	0.2970 (2)	0.3064 (3)	0.0047 (1)	0.0040 (1)	0.0132 (3)	0.0011 (2)	−0.0109 (2)	−0.0038 (3)
C11	0.0000 (0)	0.0385 (4)	0.2500 (0)	0.0092 (2)	0.0030 (2)	0.0126 (4)	0.0000 (0)	−0.0169 (4)	0.0000 (0)
C12A	0.0495 (5)	−0.0826 (5)	0.1145 (7)	0.0068 (3)	0.0037 (3)	0.0094 (6)	−0.0004 (6)	−0.0113 (5)	−0.0005 (8)
C12B	−0.0175 (5)	−0.0792 (5)	0.1605 (7)	0.0071 (3)	0.0036 (4)	0.0115 (6)	0.0020 (6)	−0.0132 (6)	−0.0026 (8)
C13A	−0.0136 (6)	−0.1464 (6)	0.1643 (8)	0.0080 (4)	0.0038 (4)	0.0113 (7)	−0.0019 (7)	−0.0118 (7)	−0.0015 (9)
C13B	0.0418 (6)	−0.1452 (5)	0.1222 (8)	0.0084 (4)	0.0031 (3)	0.0134 (7)	0.0017 (7)	−0.0141 (7)	−0.0028 (9)
C21	0.1121 (2)	0.2652 (2)	0.2865 (3)	0.0047 (1)	0.0030 (1)	0.0101 (3)	0.0005 (2)	−0.0093 (2)	−0.0004 (4)
C22	0.2611 (2)	0.2842 (3)	0.2167 (4)	0.0049 (1)	0.0049 (2)	0.0142 (4)	0.0007 (3)	−0.0109 (3)	−0.0030 (5)
C23	0.2911 (3)	0.2644 (3)	0.2998 (4)	0.0056 (2)	0.0059 (2)	0.0171 (4)	0.0017 (4)	−0.0133 (3)	−0.0044 (6)
C24	0.1752 (3)	0.3282 (3)	0.4892 (4)	0.0074 (2)	0.0051 (2)	0.0161 (4)	0.0019 (3)	−0.0156 (3)	−0.0059 (5)
C25	0.1368 (3)	0.3498 (3)	0.4187 (4)	0.0061 (2)	0.0041 (2)	0.0150 (4)	0.0010 (3)	−0.0131 (3)	−0.0042 (5)
C1	0.3761 (4)	0.0594 (4)	0.1612 (6)	0.0121 (4)	0.0049 (2)	0.0228 (7)	−0.0061 (5)	−0.0151 (7)	0.0037 (8)
C2	0.2902 (4)	0.0538 (4)	0.2272 (8)	0.0154 (4)	0.0051 (3)	0.0551 (11)	0.0065 (6)	−0.0409 (8)	−0.0131 (10)
C3	0.2437 (5)	0.0093 (5)	0.3349 (8)	0.0084 (5)	0.0133 (5)	0.0338 (12)	−0.0053 (8)	−0.0005 (12)	−0.0202 (12)

Table I (*Continued*)

Atom	x	y	z	B (Å)	Atom	x	y	z	B (Å)
C4	0.2775 (5)	−0.0256 (5)	0.3832 (6)	0.0213 (5)	0.0112 (4)	0.0164 (7)	−0.0221 (6)	−0.0133 (9)	0.0040 (9)
C5	0.3658 (4)	−0.0224 (4)	0.3135 (6)	0.0220 (4)	0.0062 (3)	0.0316 (7)	−0.0069 (6)	−0.0408 (6)	0.0048 (8)
C6	0.4140 (4)	0.0210 (4)	0.2035 (6)	0.0089 (3)	0.0074 (3)	0.0226 (7)	−0.0040 (5)	−0.0140 (6)	−0.0002 (8)
H12A	0.1152 (5)	−0.0762 (5)	0.0652 (7)	5.0000	H23B	0.2635 (3)	0.2171 (3)	0.3471 (4)	5.0000
H12B	0.0362 (5)	−0.0656 (5)	0.0547 (7)	5.0000	H24A	0.1502 (3)	0.2799 (3)	0.5346 (4)	5.0000
H12'A	0.0293 (5)	−0.0634 (6)	0.0669 (7)	5.0000	H24B	0.1601 (3)	0.3663 (3)	0.5572 (4)	5.0000
H12'B	−0.0736 (5)	−0.0626 (6)	0.1870 (7)	5.0000	H25A	0.1555 (3)	0.4005 (3)	0.3826 (4)	5.0000
H13A	−0.0758 (6)	−0.1249 (5)	0.2194 (7)	5.0000	H25B	0.0727 (3)	0.3482 (3)	0.4836 (4)	5.0000
H13B	−0.0070 (6)	−0.1755 (5)	0.0902 (7)	5.0000	H1	0.4120 (5)	0.0921 (4)	0.0821 (6)	5.0000
H13'A	0.0404 (6)	−0.1777 (6)	0.0584 (8)	5.0000	H2	0.2612 (5)	0.0818 (4)	0.1971 (8)	5.0000
H13'B	0.0991 (6)	−0.1335 (6)	0.0903 (8)	5.0000	H3	0.1813 (6)	0.0013 (6)	0.3824 (9)	5.0000
H22A	0.2747 (3)	0.2432 (3)	0.1537 (4)	5.0000	H4	0.2441 (6)	−0.0550 (5)	0.4684 (7)	5.0000
H22B	0.2910 (3)	0.3298 (3)	0.1645 (4)	5.0000	H5	0.3946 (5)	−0.0526 (4)	0.3435 (6)	5.0000
H23A	0.3548 (3)	0.2583 (3)	0.2395 (4)	5.0000	H6	0.4775 (4)	0.0235 (4)	0.1553 (6)	5.0000

(d) Rh

Atom	x	y	z	$\beta_{1,1}$	$\beta_{2,2}$	$\beta_{3,3}$	$\beta_{1,2}$	$\beta_{1,3}$	$\beta_{2,3}$
Rh	0.0000 (0)	0.19119 (6)	0.2500 (0)	0.00373 (2)	0.00244 (3)	0.0079 (6)	0.00000 (0)	−0.0077 (5)	0.00000 (0)
S11	0.0176 (1)	0.0867 (1)	0.1192 (2)	0.00735 (8)	0.00269 (8)	0.0104 (1)	−0.0002 (1)	−0.0140 (1)	0.00032 (2)
S21	0.0042 (1)	0.2808 (1)	0.3870 (2)	0.00399 (6)	0.00301 (8)	0.0096 (2)	0.0009 (1)	−0.0081 (1)	−0.00237 (2)
S22	0.1484 (1)	0.2040 (1)	0.1560 (2)	0.00402 (7)	0.00379 (10)	0.0092 (2)	0.0008 (1)	−0.0077 (1)	−0.00319 (2)
O1	0.0000 (0)	−0.1926 (5)	0.2500 (0)	0.0115 (4)	0.0028 (3)	0.0144 (7)	0.0000 (0)	−0.0178 (7)	0.0000 (0)
O2	0.2684 (3)	0.3206 (4)	0.3979 (5)	0.0059 (2)	0.0059 (3)	0.0169 (5)	0.0011 (5)	−0.0153 (4)	−0.0055 (7)
N1	0.0000 (0)	−0.0399 (7)	0.2500 (0)	0.0223 (6)	0.0021 (4)	0.0256 (9)	0.0000 (0)	−0.0426 (8)	0.0000 (0)
N2	0.1691 (3)	0.2981 (4)	0.3042 (5)	0.0045 (2)	0.0035 (3)	0.0126 (5)	0.0014 (5)	−0.0113 (4)	−0.0040 (7)
C11	0.0000 (0)	0.0324 (7)	0.2500 (0)	0.0099 (4)	0.0025 (4)	0.0109 (7)	0.0000 (0)	−0.0185 (7)	0.0000 (0)
C12	0.0495 (10)	−0.0840 (9)	0.1085 (14)	0.0068 (7)	0.0011 (5)	0.0112 (13)	0.0016 (10)	−0.0116 (12)	−0.0025 (15)
C12'	−0.0189 (10)	−0.0848 (12)	0.1654 (14)	0.0051 (6)	0.0059 (10)	0.0055 (12)	−0.0002 (14)	−0.0068 (11)	0.0004 (19)
C13	0.0431 (10)	−0.1454 (10)	0.1212 (14)	0.0064 (6)	0.0028 (6)	0.0135 (13)	0.0018 (11)	−0.0134 (11)	−0.0073 (16)
C13'	−0.0108 (12)	−0.1531 (10)	0.1607 (17)	0.0097 (8)	0.0025 (6)	0.0147 (16)	−0.0059 (12)	−0.0160 (15)	0.0040 (18)
C21	0.1150 (4)	0.2663 (5)	0.2862 (6)	0.0039 (2)	0.0026 (3)	0.0090 (6)	0.0002 (5)	−0.0084 (5)	0.0008 (8)
C22	0.2636 (5)	0.2844 (6)	0.2139 (8)	0.0049 (3)	0.0051 (5)	0.0148 (8)	−0.0001 (6)	−0.0122 (6)	−0.0018 (10)
C23	0.2901 (5)	0.2649 (6)	0.3015 (8)	0.0052 (3)	0.0051 (5)	0.0169 (8)	0.0008 (7)	−0.0138 (6)	−0.0024 (11)
C24	0.1759 (5)	0.3290 (6)	0.4890 (8)	0.0064 (3)	0.0046 (4)	0.0136 (7)	0.0027 (6)	−0.0133 (6)	−0.0062 (9)
C25	0.1405 (5)	0.3526 (5)	0.4133 (7)	0.0050 (3)	0.0037 (4)	0.0133 (7)	0.0022 (6)	−0.0120 (6)	−0.0058 (9)
C1	0.3793 (8)	0.0553 (8)	0.1672 (11)	0.0129 (6)	0.0051 (5)	0.0252 (14)	−0.0073 (10)	−0.0226 (12)	0.0067 (15)
C2	0.2915 (9)	0.0564 (8)	0.2300 (14)	0.0314 (7)	0.0042 (5)	0.0853 (18)	0.0105 (11)	−0.0934 (12)	−0.0169 (18)
C3	0.2465 (11)	0.0104 (11)	0.3483 (24)	0.0116 (10)	0.0105 (8)	0.0989 (46)	0.0076 (16)	−0.0369 (29)	−0.0433 (29)
C4	0.2786 (10)	−0.0297 (8)	0.3832 (14)	0.0165 (10)	0.0097 (6)	0.0147 (18)	−0.0209 (11)	0.0129 (23)	−0.0087 (17)
C5	0.3623 (9)	−0.0251 (8)	0.3207 (11)	0.0252 (8)	0.0055 (6)	0.0249 (11)	−0.0071 (13)	−0.0402 (12)	0.0059 (15)
C6	0.4156 (7)	0.0176 (9)	0.2072 (11)	0.0088 (5)	0.0093 (8)	0.0249 (14)	−0.0016 (12)	−0.0194 (11)	0.0000 (19)

Atom	x	y	z	B (Å)	Atom	x	y	z	B (Å)
H12A	0.0454 (8)	−0.0567 (7)	0.0430 (11)	5.0000	H23B	0.2612 (4)	0.2182 (5)	0.3518 (6)	5.0000
H12B	0.1067 (8)	−0.0972 (7)	0.0714 (11)	5.0000	H24A	0.1494 (4)	0.2828 (4)	0.5371 (6)	5.0000
H12'A	−0.0814 (8)	−0.1054 (10)	0.2266 (11)	5.0000	H24B	0.1614 (4)	0.3685 (4)	0.5562 (6)	5.0000
H12'B	−0.0115 (8)	−0.0586 (10)	0.0912 (11)	5.0000	H25A	0.1605 (4)	0.4012 (4)	0.3758 (6)	5.0000
H13A	0.0972 (8)	−0.1247 (8)	0.0905 (12)	5.0000	H25B	0.0759 (4)	0.3514 (4)	0.4793 (6)	5.0000
H13B	0.0478 (8)	−0.1728 (8)	0.0475 (12)	5.0000	H1	0.4178 (6)	0.0862 (6)	0.0899 (9)	5.0000
H13'A	−0.0040 (10)	−0.1829 (8)	0.0951 (13)	5.0000	H2	0.2667 (6)	0.0897 (6)	0.1958 (10)	5.0000
H13'B	−0.0766 (10)	−0.1353 (8)	0.2271 (13)	5.0000	H3	0.1885 (7)	0.0069 (8)	0.3782 (13)	5.0000
H22A	0.2776 (4)	0.2450 (5)	0.1526 (6)	5.0000	H4	0.2434 (8)	−0.0618 (6)	0.4639 (10)	5.0000
H22B	0.2938 (4)	0.3304 (5)	0.1656 (6)	5.0000	H5	0.3920 (7)	−0.0522 (6)	0.3514 (8)	5.0000
H23A	0.3539 (4)	0.2567 (5)	0.2420 (6)	5.0000	H6	0.4791 (5)	0.0180 (7)	0.1568 (8)	5.0000

(e) Ir

Atom	x	y	z	$\beta_{1,1}$	$\beta_{2,2}$	$\beta_{3,3}$	$\beta_{1,2}$	$\beta_{1,3}$	$\beta_{2,3}$
Ir	0.0000 (0)	0.19044 (5)	0.2500 (0)	0.00364 (2)	0.00259 (2)	0.0071 (4)	0.00000 (0)	−0.0067 (3)	0.00000 (0)
S11	0.0166 (2)	0.0857 (2)	0.1206 (2)	0.00735 (11)	0.0030 (1)	0.0099 (2)	0.0001 (2)	−0.0134 (2)	0.00022 (3)
S21	0.0047 (2)	0.2807 (2)	0.3859 (3)	0.00398 (9)	0.0031 (1)	0.0092 (2)	0.0012 (2)	−0.0075 (2)	−0.00249 (3)
S22	0.1490 (2)	0.2027 (2)	0.1570 (2)	0.00395 (9)	0.0040 (1)	0.0099 (2)	0.0009 (2)	−0.0079 (2)	−0.00296 (3)
O1	0.0000 (0)	−0.1939 (7)	0.2500 (0)	0.0106 (5)	0.0025 (4)	0.0145 (*)	0.0000 (0)	−0.0167 (*)	0.0000 (0)
O2	0.2674 (4)	0.3201 (6)	0.3992 (7)	0.0060 (3)	0.0053 (4)	0.0165 (7)	0.0018 (6)	−0.0150 (5)	−0.0050 (1)
N1	0.0000 (0)	−0.0414 (9)	0.2500 (0)	0.0252 (10)	0.0016 (5)	0.0219 (*)	0.0000 (0)	−0.0411 (*)	0.0000 (0)
N2	0.1694 (5)	0.2994 (6)	0.3033 (7)	0.0044 (3)	0.0047 (4)	0.0129 (7)	0.0006 (7)	−0.0115 (5)	−0.0032 (1)
C11	0.0000 (0)	0.0309 (10)	0.250 (0)	0.0084 (7)	0.0027 (7)	0.0150 (1)	0.0000 (0)	−0.017 (*)	0.0000 (0)
C12A	0.0429 (16)	−0.0813 (12)	0.113 (2)	0.0106 (12)	0.0011 (7)	0.0115 (2)	−0.0055 (14)	−0.013 (*)	−0.0023 (2)
C12B	−0.0236 (15)	−0.0896 (18)	0.169 (2)	0.0062 (10)	0.0071 (15)	0.0076 (2)	−0.0039 (21)	−0.010 (*)	0.0055 (3)
C13A	−0.0085 (12)	−0.1542 (11)	0.157 (2)	0.0089 (8)	0.0014 (6)	0.0151 (2)	−0.0079 (11)	−0.018 (*)	0.0026 (2)
C13B	0.0461 (13)	−0.1379 (14)	0.120 (2)	0.0057 (8)	0.0040 (9)	0.0139 (2)	−0.0004 (14)	−0.013 (*)	−0.0089 (2)
C21	0.1159 (6)	0.2656 (6)	0.285 (1)	0.0033 (4)	0.0021 (4)	0.0101 (1)	0.0016 (7)	−0.006 (8)	−0.0001 (1)
C22	0.2644 (7)	0.2846 (8)	0.214 (1)	0.0044 (4)	0.0058 (7)	0.0145 (1)	0.0012 (9)	−0.010 (9)	−0.0049 (1)
C23	0.2901 (7)	0.2627 (9)	0.302 (1)	0.0052 (4)	0.0056 (6)	0.0148 (1)	0.0013 (10)	−0.013 (9)	−0.0045 (1)
C24	0.1752 (8)	0.3297 (9)	0.489 (1)	0.0070 (5)	0.0077 (8)	0.0127 (1)	0.0040 (11)	−0.013 (9)	−0.0092 (2)
C25	0.1391 (7)	0.3499 (7)	0.415 (1)	0.0067 (4)	0.0033 (5)	0.0164 (1)	0.0003 (8)	−0.016 (8)	−0.0065 (1)
C1	0.3791 (11)	0.0563 (10)	0.170 (2)	0.0106 (9)	0.0056 (7)	0.0195 (2)	−0.0071 (13)	−0.012 (*)	−0.0023 (2)
C2	0.2950 (12)	0.0570 (11)	0.222 (2)	0.0222 (10)	0.0046 (8)	0.0582 (3)	0.0017 (17)	−0.059 (*)	−0.0039 (3)
C3	0.2488 (15)	0.0092 (15)	0.339 (2)	0.0101 (14)	0.0125 (14)	0.0368 (4)	−0.0017 (25)	−0.004 (*)	−0.0227 (3)
C4	0.2748 (14)	−0.0314 (11)	0.392 (2)	0.0230 (12)	0.0142 (9)	0.0122 (2)	−0.0332 (13)	−0.006 (*)	0.0061 (2)
C5	0.3598 (13)	−0.0261 (10)	0.326 (1)	0.0305 (11)	0.0061 (8)	0.0283 (1)	−0.0131 (16)	−0.051 (*)	0.0123 (2)
C6	0.4153 (10)	0.0143 (12)	0.211 (2)	0.0086 (7)	0.0098 (11)	0.0280 (2)	0.0046 (16)	−0.021 (*)	−0.0112 (3)

Atom	x	y	z	B (A)	Atom	x	y	z	B (A)
H12A	0.0366 (16)	−0.0531 (12)	0.051 (2)	5.0000	H23B	0.2595 (7)	0.2172 (9)	0.352 (1)	5.0000
H12B	0.1051 (16)	−0.0904 (12)	0.066 (2)	5.0000	H24A	0.1480 (8)	0.2834 (9)	0.539 (1)	5.0000
H12'A	−0.0811 (15)	−0.1133 (18)	0.229 (2)	5.0000	H25A	0.1604 (8)	0.3690 (9)	0.555 (1)	5.0000
H12'B	−0.0188 (15)	−0.0625 (18)	0.095 (2)	5.0000	H25B	0.0751 (7)	0.3482 (7)	0.481 (1)	5.0000
H13A	0.0145 (12)	−0.1845 (11)	0.075 (2)	5.0000	H1	0.4181 (11)	0.0905 (10)	0.093 (2)	5.0000
H13B	−0.0703 (12)	−0.1434 (11)	0.204 (2)	5.0000	H2	0.2697 (12)	0.0852 (11)	0.186 (2)	5.0000
H13'A	0.0962 (13)	−0.1125 (14)	0.104 (2)	5.0000	H3	0.1856 (15)	0.0074 (15)	0.388 (2)	5.0000
H13'B	0.0647 (13)	−0.1632 (14)	0.035 (2)	5.0000	H4	0.2361 (14)	−0.0632 (11)	0.472 (2)	5.0000
H22A	0.2783 (7)	0.2444 (8)	0.149 (1)	5.0000	H5	0.3845 (13)	−0.0535 (10)	0.364 (1)	5.0000
H22B	0.2964 (7)	0.3292 (8)	0.161 (1)	5.0000	H6	0.4787 (10)	0.0126 (12)	0.160 (2)	5.0000
H23A	0.3534 (7)	0.2543 (9)	0.243 (1)	5.0000					

[a] The form of the anisotropic thermal parameter is: $\exp[-(\beta_{1,1}h^2 + \beta_{2,2}k^2 + \beta_{3,3}l^2 + \beta_{1,2}hk + \beta_{1,3}hl + \beta_{2,3}kl)](\times 10)$.

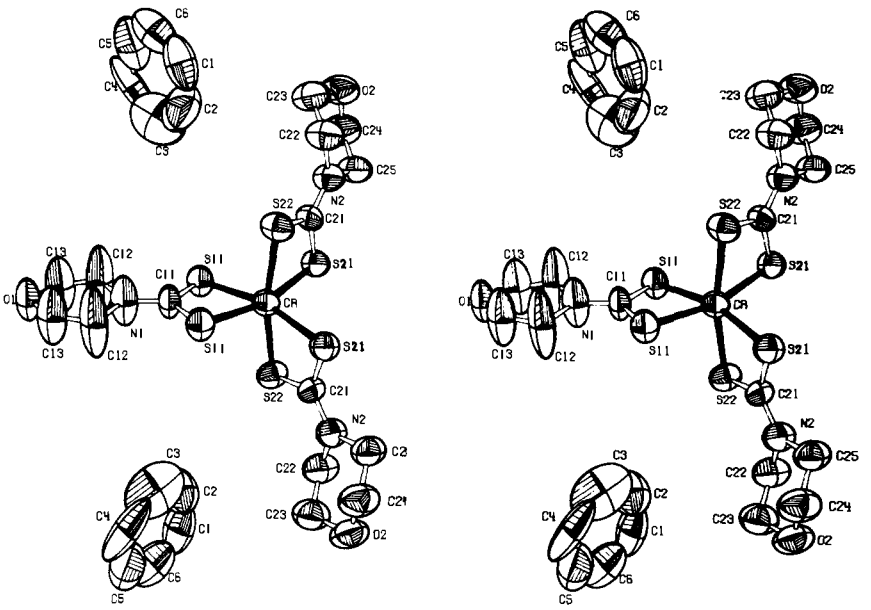

Figure 1. Stereoscopic pair view of CrMBz. Disorder not shown, to minimize crowding.

Table II. Interatomic Distances for M(MBz) (Å)

	M = Cr	M = Fe	M = Co	M = Rh	M = Ir
M–S11	2.396 (3)	2.315 (1)	2.272 (1)	2.363 (4)	2.364 (3)
M–S21	2.406 (3)	2.323 (1)	2.277 (1)	2.370 (4)	2.375 (3)
M–S22	2.386 (3)	2.313 (1)	2.270 (1)	2.361 (3)	2.376 (3)
S11–C11	1.707 (8)	1.713 (1)	1.709 (2)	1.73 (1)	1.724 (9)
S21–C21	1.73 (1)	1.713 (1)	1.718 (3)	1.72 (1)	1.73 (1)
S22–C21	1.69 (1)	1.719 (1)	1.715 (2)	1.73 (1)	1.71 (1)
C11–N1	1.32 (1)	1.311 (3)	1.314 (5)	1.31 (2)	1.31 (2)
C21–N2	1.33 (1)	1.327 (2)	1.322 (3)	1.32 (1)	1.34 (1)
N1–C12A	1.63 (7)	1.562 (5)	1.579 (7)	1.60 (4)	1.53 (3)
N1–C12B	1.48 (5)	1.543 (5)	1.543 (7)	1.53 (4)	1.59 (4)
C12A–C13A	1.42 (11)	1.503 (7)	1.50 (1)	1.11 (5)	1.54 (3)
C12B–C13B	1.59 (8)	1.500 (7)	1.50 (1)	1.24 (5)	1.40 (4)
C13A–O1	1.50 (8)	1.454 (6)	1.46 (1)	1.52 (5)	1.44 (3)
C13B–O1	1.46 (8)	1.485 (6)	1.50 (1)	1.43 (6)	1.62 (4)
N2–C22	1.45 (1)	1.470 (2)	1.468 (3)	1.47 (1)	1.48 (1)
N2–C25	1.47 (1)	1.473 (2)	1.476 (3)	1.47 (1)	1.44 (1)
C22–C23	1.46 (1)	1.493 (2)	1.485 (4)	1.49 (2)	1.50 (2)
C24–C25	1.44 (1)	1.480 (2)	1.484 (4)	1.51 (2)	1.49 (1)
C23–O2	1.42 (1)	1.429 (2)	1.429 (3)	1.41 (1)	1.43 (1)
C24–O2	1.41 (1)	1.435 (2)	1.429 (3)	1.43 (1)	1.42 (1)
C1–C2	1.30 (3)	1.349 (6)	1.345 (8)	1.37 (4)	1.34 (3)
C2–C3	1.28 (3)	1.339 (6)	1.333 (9)	1.42 (5)	1.43 (4)
C3–C4	1.20 (7)	1.30 (1)	1.28 (1)	1.19 (8)	1.27 (7)
C4–C5	1.40 (6)	1.363 (9)	1.36 (1)	1.30 (6)	1.32 (5)
C5–C6	1.34 (3)	1.342 (5)	1.337 (7)	1.36 (4)	1.35 (3)
C6–C1	1.30 (3)	1.304 (7)	1.306 (7)	1.27 (4)	1.32 (3)

of the solvate, indicating that the differences in lattice forces, imposed by inclusion of the different solvents in the crystal, are not too great. In each case, there is a significant increase in ⟨M–L⟩ from $3d^6$ (t_2^6) and $4d^6$: 0.092 (4) Å between CoMBz (2.273 (1) Å) and RhMBz (2.365 (4) Å) or 0.093 Å averaged over the two pairs of analogous compounds of known structure. On the other hand, there is little difference between the known $4d^6$ and $5d^6$ analogues: 0.007 (4) Å between RhMBz and IrMBz (2.372 (3) Å).

The structural data confirm the previous observation[7,8] (Table VI) that the increase in ⟨M–L⟩ between complexes within the same transition series is mainly due to an increase in the number of unpaired electrons in the t^2 subshell: ⟨M–S⟩ decreases by 0.131 Å from $Cr(S_2CNC_4H_8O)_3 \cdot CH_2Cl_2$ with three unpaired electrons (t_2^3) to $Co(S_2CNC_4H_8O)_3 \cdot CH_2Cl_2$ with three more electrons, but all paired (t_2^6). However, there is only a slight increase in

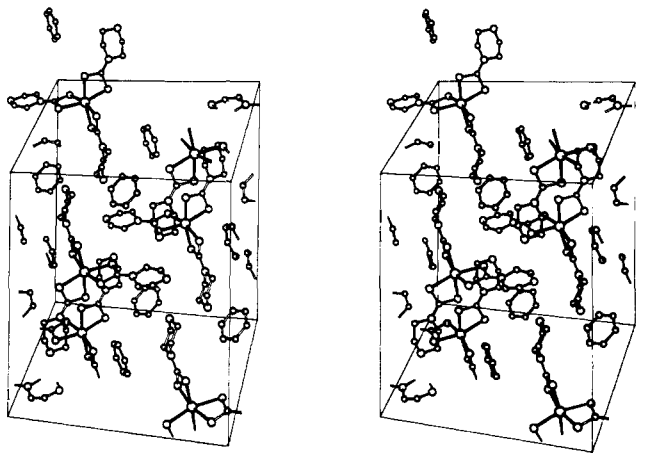

Figure 2. Molecular packing in CrMBz.

⟨M–L⟩ (0.03 Å) on adding two unpaired electrons to the e subshell from t_2^3 in CrPDC to $t_2^3e^2$ in FePDC.[8] The IrMBz complex is the closest to octahedral of the MBz series, and FeMBz has the most distortion from octahedral geometry. The average "bite angle" of the ligand ⟨S–M–S⟩ tends to increase as ⟨M–L⟩ decreases over the data available so far. This angle is therefore essentially independent of the d-electron configuration. These complexes and related tris(dithiocarbamates) all have structural features in common: all are approximately trigonally distorted octahedra with small deviations from D_3 symmetry arising from lattice forces which vary due to packing of complex and solvent molecules in the crystal, from Jahn–Teller distortion in Mn(III) complexes, and, in the present series, from crystallographic symmetry, which imposes a C_2 axis over the D_3 geometry.

Magnetic Properties. The temperature dependence of the magnetic moments of the benzene (FeMBz) and dichloromethane (FeMDc) solvated and unsolvated (FeM) analogues of $Fe(S_2CNC_4H_8O)_3$ are given in Table VII and Figure 3. The relative values of the magnetic moments are considered to be accurate to 0.1%, the absolute values somewhat less. Some of the moment values were much less accurate due to temperature instability, and these are omitted from the figure and are given to only two decimal places in the table. The magnetic properties show major differences

Table III. Interatomic Angles for M(MBz) (deg)

	M = Cr	M = Fe	M = Co	M = Rh	M = Ir
S11–M–S11'	74.2 (2)	75.52 (2)	76.48 (3)	74.2 (2)	73.3 (1)
S11–M–S21	164.2 (1)	164.63 (1)	166.93 (3)	166.9 (1)	167.02 (9)
S11'–M–S21	94.93 (9)	93.79 (1)	94.29 (2)	96.6 (1)	97.45 (9)
S11–M–S22	95.0 (1)	94.44 (1)	94.66 (3)	96.8 (1)	97.4 (1)
S11'–M–S22	95.4 (1)	96.35 (1)	94.38 (3)	92.2 (1)	91.2 (1)
S21–M–S21'	97.9 (2)	98.68 (2)	96.22 (4)	94.0 (2)	93.1 (1)
S21–M–S22	74.3 (1)	75.53 (1)	76.60 (2)	73.9 (1)	73.30 (9)
S21'–M–S22	97.0 (1)	95.45 (1)	95.61 (3)	98.2 (1)	99.1 (1)
S22–M–S22'	167.0 (2)	166.35 (2)	168.48 (4)	168.7 (2)	169.3 (2)
M–S11–C11	85.1 (5)	86.40 (6)	86.4 (1)	87.4 (5)	88.5 (4)
M–S21–C21	84.2 (4)	86.24 (4)	86.31 (8)	87.2 (4)	87.6 (4)
M–S22–C21	85.8 (4)	86.43 (5)	86.60 (9)	87.4 (4)	87.9 (3)
S11–C11–N1	122.2 (5)	124.16 (6)	124.7 (1)	124.5 (5)	125.1 (4)
S11–C11–S11'	115.6 (9)	111.7 (1)	110.7 (2)	111 (1)	109.8 (9)
C11–N1–C12A	123 (3)	122.0 (2)	122.3 (3)	120 (1)	118 (1)
C11–N1–C12B	119 (2)	120.3 (2)	120.9 (3)	122 (2)	123 (1)
C12A–N1–C12A'	114 (5)	116.0 (4)	115.3 (5)	120 (2)	123 (2)
C12B–N1–C12B'	122 (4)	119.5 (4)	118.1 (5)	116 (3)	113 (3)
N1–C12A–C13A	95 (5)	98.75 (4)	99.0 (5)	113 (3)	103 (2)
N1–C12B–C13B	102 (4)	99.7 (4)	100.1 (6)	119 (4)	92 (3)
C12A–C13A–O1	107 (4)	104.9 (4)	104.7 (7)	130 (4)	110 (3)
C12B–C13B–O1	107 (5)	106.5 (4)	105.2 (7)	123 (4)	100 (3)
C13A–O1–C13A'	107 (7)	114.6 (5)	115.5 (7)	112 (3)	120 (2)
C13B–O1–C13B'	118 (5)	114.7 (5)	114.6 (7)	120 (3)	102 (2)
S21–C21–N2	121.3 (9)	125.4 (1)	125.5 (2)	125.3 (9)	124.3 (8)
S22–C21–N2	123.1 (9)	122.9 (1)	124.2 (2)	123.3 (9)	124.5 (7)
C21–N2–C22	123 (1)	123.6 (1)	123.0 (2)	123 (1)	122.1 (9)
C21–N2–C25	125 (1)	122.9 (1)	122.8 (2)	123 (1)	123.2 (9)
C22–N2–C25	112.1 (9)	113.5 (1)	114.2 (2)	113.8 (9)	114.6 (8)
N2–C22–C23	112 (1)	108.8 (1)	109.3 (2)	108 (1)	109.1 (9)
N2–C25–C24	113 (1)	109.1 (1)	109.4 (2)	108 (1)	110.7 (9)
C22–C23–O2	113 (1)	110.6 (2)	111.3 (3)	112 (1)	110 (1)
C25–C24–O2	114 (1)	112.1 (1)	112.7 (2)	112 (1)	113.5 (9)
C23–O2–C24	110 (1)	108.3 (1)	109.2 (2)	109 (1)	109.2 (8)
C2–C1–C6	122 (4)	120.0 (4)	120.0 (6)	125 (3)	127 (2)
C3–C2–C1	115 (4)	117.9 (6)	118.5 (8)	110 (4)	107 (3)
C2–C3–C4	133 (5)	122.4 (8)	123 (1)	127 (5)	132 (4)
C3–C4–C5	111 (4)	119.8 (6)	117.9 (9)	119 (4)	113 (3)
C4–C5–C6	122 (4)	117.6 (7)	120.3 (7)	122 (4)	125 (3)
C5–C6–C1	117 (3)	122.3 (6)	120.0 (6)	117 (3)	116 (2)

Table IV. Closest Intermolecular Contacts (Å)

Molecule 1	Molecule 2	Cr	Fe	Co	Rh	Ir	Symmetry operation		
S11	C12B	3.47 (2)	3.461 (5)	3.480 (6)	3.50 (2)	3.46 (2)	$-x$	$-y$	$-z$
	C12A	3.83 (3)	3.855 (5)	3.822 (6)	3.71 (3)	3.68 (3)	$-x$	$-y$	$-z$
	C13A	3.69 (3)	3.684 (6)	3.683 (9)	3.77 (4)	3.71 (3)	$-x$	$-y$	$-z$
S22	C22	3.87 (1)	3.784 (2)	3.776 (3)	3.78 (1)	3.76 (1)	$0.5-x$	$0.5-y$	$-z$
	S22	3.79 (1)	3.812 (1)	3.865 (1)	3.81 (1)	3.816 (5)	$0.5-x$	$0.5-y$	$-z$
O1	O2	3.67 (1)	3.669 (1)	3.642 (2)	3.68 (2)	3.690 (7)	$-0.5+x$	$-0.5+y$	z
	C23	3.78 (1)	3.772 (2)	3.742 (3)	3.78 (2)	3.80 (1)	$-0.5+x$	$-0.5+y$	z
	C24	3.93 (2)	3.859 (2)	3.831 (4)	3.83 (2)	3.80 (2)	x	$-y$	$-0.5+z$
O2	O2	3.36 (2)	3.356 (3)	3.337 (5)	3.34 (3)	3.31 (2)	$0.5-x$	$0.5-y$	$1-z$
	C23	3.54 (1)	3.515 (2)	3.515 (4)	3.50 (2)	3.45 (1)	$0.5-x$	$0.5-y$	$1-z$
	C13A	3.51 (4)	3.453 (6)	3.405 (9)	3.42 (5)	3.47 (4)	$0.5+x$	$0.5+y$	z
	C24	3.50 (2)	3.449 (2)	3.464 (4)	3.52 (2)	3.52 (2)	$0.5-x$	$0.5-y$	$1-z$
	C13B	3.53 (3)	3.531 (6)	3.526 (9)	3.58 (4)	3.56 (3)	$0.5-x$	$0.5+y$	$0.5-z$
	C12B	3.90 (4)	3.807 (4)	3.748 (9)	3.67 (4)	3.61 (4)	$0.5+x$	$0.5+y$	z
C13A	C23	3.53 (5)	3.480 (6)	3.428 (9)	3.45 (4)	3.49 (3)	$0.5+x$	$0.5+y$	z
C23	C24	3.49 (2)	3.421 (3)	3.446 (5)	3.48 (3)	3.46 (2)	$0.5-x$	$0.5-y$	$1-z$

Table V. Contacts between Complex and Included Benzene Molecules (Å)

Molecule 1	Molecule 2	Cr	Fe	Co	Rh	Ir	Symmetry operation		
C3	C12A	3.56 (5)	3.472 (7)	3.45 (1)	3.55 (5)	3.53 (4)	x	$-y$	$0.5+z$
	C25	3.90 (4)	3.841 (7)	3.817 (9)	3.72 (4)	3.80 (3)	$0.5-x$	$-0.5+y$	$0.5-z$
C4	N2	3.80 (4)	3.675 (7)	3.683 (9)	3.64 (5)	3.62 (4)	$0.5-x$	$-0.5+y$	$0.5-z$
	C25	3.90 (4)	3.753 (7)	3.747 (9)	3.63 (3)	3.72 (2)	$0.5-x$	$-0.5+y$	$0.5-z$
	C22	3.88 (4)	3.784 (7)	3.820 (8)	3.83 (4)	3.82 (3)	$0.5-x$	$-0.5+y$	$0.5-z$
C5	C25	3.72 (3)	3.686 (5)	3.672 (6)	3.64 (2)	3.70 (2)	$0.5-x$	$-0.5+y$	$0.5-z$
	N2	3.70 (3)	3.725 (5)	3.743 (5)	3.75 (2)	3.73 (2)	$0.5-x$	$-0.5+y$	$0.5-z$
C6	C25	3.81 (3)	3.766 (5)	3.780 (5)	3.74 (2)	3.79 (2)	$0.5-x$	$-0.5+y$	$0.5-z$

Table VI. Coordination Sphere Data for Some Dithiocarbamate Complexes

Compound	⟨M–S⟩, Å	⟨δ⟩, deg	γ	ζ	ζ′	⟨C–N⟩	Space group	R factor	Ref
CrMBz	2.396	74.3	165.1	95.6	96.1	1.33	C2/c	0.032	a
FeMBz	2.318	75.5	165.2	95.6	97.1	1.32	C2/c	0.047	a
CoMBz	2.273	76.6	167.4	94.8	95.2	1.32	C2/c	0.036	a
RhMBz	2.365	74.0	167.5	95.7	95.9	1.32	C2/c	0.054	a
IrMBz	2.372	73.3	167.8	95.9	96.0	1.33	C2/c	0.050	a
CrMDc	2.406	73.8	162.0	94.6	99.6	1.35	$P\bar{1}$	0.043	7
MnMBz	2.461	72.3	158.5	94.5	102.6	1.33	$P\bar{1}$	0.040	7
FeMDc	2.430	72.5	157.3	93.6	104.5	1.31	$P\bar{1}$	0.063	6
CoMDc	2.275	76.1	165.4	94.2	97.1	1.33	$P\bar{1}$	0.044	6
RhMDc	2.369	73.5	165.5	96.6	94.8	1.33	$P\bar{1}$	0.043	7
FePDc[b]	2.407	74.5	161.0	93.4	101.7	1.31	$P2_1/n$	0.13	2
$FePDc(C_6H_6)_{0.5}$	2.434	73.3	160.6	94.2	101.3	1.32	$P2_1/n$	0.045	8
$CrPDc(C_6H_6)_{0.5}$	2.404	74.2	164.1	95.1	97.5	1.34	$P2_1/n$	0.044	8
$IrPDc(C_6H_6)_{0.5}$	2.376	73.3	167.2	97.4	92.8	1.32	$P2_1/n$	0.064	8

[a] Present work. [b] Tris(1-pyrrolidinecarbodithioato-S,S′) complexes abbreviated as PDc.

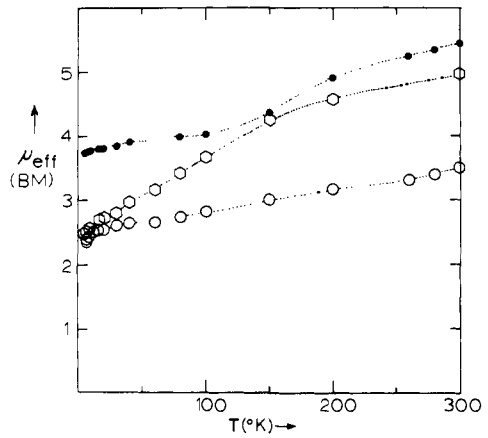

Figure 3. Temperature dependence of magnetic moments (μ_{eff}, μ_B) of: O, FeMBz; ○, FeMDc; ●, FeM (from FeMDc) (FeM from FeMBz omitted to minimize crowding).

Table VII. Magnetic Moments (μ_{eff}, μ_B) for Iron(III) Complexes

T, °C	FeMBz	FeMDc[a]	FeM[b]	FeM[c]
5	2.342	3.738	2.453	2.310
6	2.390	3.75	2.516	2.330
7	2.412	3.76	2.538	2.338
8	2.414	3.748	2.539	
9	2.434	3.746	2.565	2.344
10		3.785	2.82	
13	2.538	3.83		
16	2.536	3.802	2.698	2.465
20	2.546	3.807	2.730	2.507
30	2.609	3.859	2.804	
40	2.647	3.900	2.968	2.798
60	2.650	3.829	3.162	3.109
80	2.751	3.991	3.419	3.492
100	2.821	4.070	3.671	3.851
150	3.017	4.331	4.203	4.536
200	3.169	4.918	4.572	
260	3.320	5.249		
280	3.409	5.347		
300	3.526	5.453	4.964	

[a] Dichloromethane solvated complex. [b] Unsolvated complex, from dichloromethane solvate. [c] Unsolvated complex, from benzene solvate.

depending on the solvate or lack of it, though in each case the moment rises with increasing temperature. FeM appears to be the same based on magnetic and infrared spectral data, whether produced by removal of solvent from FeMBz or FeMDc. Given the relatively small structural differences between FeMBz and FeMDc, the difference in their magnetism is especially dramatic, but it does indicate that a similar structure for FeM to those of FeMBz and FeMDc is at least reasonable.

From the low temperature limits of their moments, it is clear that FeMBz and FeM both have low spin ground states, which must consist of $^2T_2$ states, split by the trigonal distortion. However, in FeMDc the low temperature limit of the moment clearly indicates an $S = \frac{3}{2}$ ground state, which must arise from the $^4T_1$ state, also split ($^4A_2$ and ^4E) by distortion, as indicated in **1**. A similar $S = \frac{3}{2}$ ground state is also probable in a tris(1-pyrrolidinecarbodithioato-S,S′) analogue.[15] Similar behavior is observed in presumably octahedral iron(II) complexes, where distortion splitting also lowers an intermediate spin to ground state, as in **2**.[4] The much greater splitting of $^4T_1$ than of $^2T_2$ in **1**, requires tetragonal distortion, which should therefore be directly observable in a crystal structure of FeMDc at low temperatures, where the complex is predominantly in the quartet state.

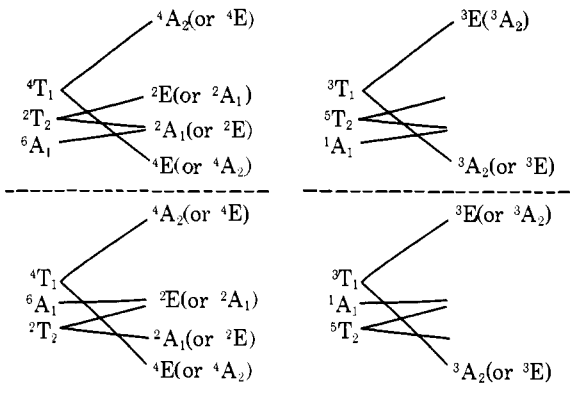

1 2

Removal of the solvent from FeMDc to form FeM produces a "normal" high spin–low spin crossover, but, in view of the probable structural similarity between FeM and FeMDc, a relatively low lying quartet state seems likely in FeM also.

A doublet ground state is clearly indicated by the low temperature limit of the moment of FeMBz. The moment rises with increasing temperature, but the highest value (3.5 μ_B at 300 K) is lower than the expected value (~3.8 μ_B) for a quartet state. The moment is still rising at this temperature (Figure 3) but, at higher temperatures, the rise in moment cannot safely be attributed to the spin state equilibrium, since decomposition to FeM would also produce a rise in moment. Thus, the magnetic properties of FeMBz are accountable in terms of a doublet ⇌ sextet, a doublet ⇌ quartet ⇌ sextet, or possibly a doublet ⇌ quartet spin state equilibrium. Assuming room temperature μ_{eff}^2 values of 5, 14, and 35 μ_B for the doublet, quartet, and sextet spin states, respectively, and assuming further that only two spin

states contribute significantly to each complex, the room temperature populations can be described as approximately as 75% sextet and 25% quartet in FeMDc, 65% sextet and 35% doublet in FeM (from dichloromethane), 25% sextet and 75% doublet or 83% quartet and 17% doublet in FeMBz. In any case, observations of $S = 3/2$ ground states in homogeneously liganded iron(III) are unique to FeMDc and FePDc.

The existence of low lying triplets also seems likely in other complexes of the dithiocarbamate type (Table VI) and this would significantly affect the temperature dependence of the moments and would explain the difficulty in fitting the data for many dithiocarbamates[1] to a model in which only doublet and sextet states were considered. It may also be one reason why the ⟨Fe-S⟩ vs. μ_{eff} plot fails to fit well to a line or curve.

The large difference in ⟨Fe-S⟩ (0.12 Å) between FeMBz and FeMDc is surprising when compared with the magnetic data. It appears from the data already collected on the effects of electron pairing in such systems (Table VI) that ⟨Fe-S⟩ for the proposed quartet state must be greater than that for the doublet but less than for the sextet state. In particular, ⟨Fe-S⟩ for the pure doublet state in FeMBz must be less than the observed value, while ⟨Fe-S⟩ for the pure sextet state in FeMDc must be greater than that observed. Therefore the change in ⟨Fe-S⟩ from low spin (distortion split $^2T_2$) (in FeMBz) to high spin ($^6A_1$) (in FeMDc) must be greater than 0.12 Å, and markedly greater than the 0.1 Å estimated for the group of complexes in general.[1]

The differences between the moments of the unsolvated FeM from FeMDc and FeMBz are too large to attribute to experimental inaccuracy. However, given the large changes in magnetism produced by small changes in packing, only a very small difference between the two forms of FeM would account for the observations.

At this stage the changes in electronic state of the iron system can only be attributed to lattice forces. If some specific interaction mechanism with the included solvent, such as hydrogen bonding of a ligand sulfur atom with CH_2Cl_2[6,7] or $CHCl_3$,[17] causes the changes in electronic state, this is not yet evident because insufficient structural data exist or possibly because no such mechanism exists. Studies now in progress may resolve this question.

The infrared data in Table VIII lists the region of interest: the metal-sulfur stretch. One peak is observed for each of the complexes except for those of iron(III), where the plurality of peaks is compatible with (but inconclusive about) equilibria between more than one spin state. These data are also compatible with the pressure data on high spin and low spin Fe-S stretches in other ferric dithiocarbamates in which the relative intensities follow the expected spin state concentrations.[18] The resolution in present compounds is less than optimal, especially for FeM, where individual peaks could not be resolved unambiguously. The small differences between the bands in CrMBz and CrMDc, for example, are real, indicating that there is a small effect of the solvent in the lattice and that more data are needed on other compounds before a detailed interpretation of the Fe-S region is made. It seems likely, from the structural and magnetic studies presented here, that almost any of the possible spin states in the iron(III) system can be isolated by crystallization of tris(4-morpholinecarbodithioato-*S,S'*)iron(III) with suitable solvents, and this method is a valuable one for the study of the relation of structure to spin state and the nature and mechanism of spin state equilibria.

Table VIII. Metal–Ligand Stretching Region (cm^{-1})

	MBz	MDc	Unsolved: From CH_2Cl_2	Unsolved: From C_6H_6
Cr	361	364		
Fe	326 (sh), 332, 336	327, 332, 335	330–340	330–340
Co	365	362		
Rh	339	341		
Ir	318			

Acknowledgment. Support received for instrumentation under NSF Grant No. GP-41679 is gratefully acknowledged.

Supplementary Material Available: a listing of observed structure factors (66 pages). Ordering information is given on any current masthead page.

References and Notes

(1) A. H. Ewald, R. L. Martin, E. Sinn, and A. H. White, *Inorg. Chem.*, **8**, 1837 (1969), and references cited therein.
(2) P. C. Healy and A. H. White, *Chem. Commun.*, 1446 (1971); *J. Chem. Soc., Dalton Trans.*, 1163 (1972).
(3) J. G. Leipoldt and P. Coppens, *Inorg. Chem.*, **12**, 2269 (1973).
(4) A. J. Cunningham, J. E. Fergusson, H. K. J. Powell, E. Sinn, and H. Wong, *J. Chem. Soc., Dalton Trans.*, 2155 (1972).
(5) R. M. Golding, P. C. Healy, P. W. G. Newman, E. Sinn, and A. H. White, *Inorg. Chem.*, **11**, 2435 (1972); E. Sinn, Thesis, University of Sydney, 1964.
(6) P. C. Healy and E. Sinn, *Inorg. Chem.*, **14**, 109 (1975).
(7) R. J. Butcher and E. Sinn, *J. Chem. Soc., Dalton Trans.*, 2517 (1975).
(8) E. Sinn, *Inorg. Chem.*, **15**, 369 (1976).
(9) P. W. R. Corfield, R. J. Doedens, and J. A. Ibers, *Inorg. Chem.*, **6**, 197 (1967).
(10) D. T. Cromer and J. T. Waber, *Acta Crystallogr.*, **18**, 511 (1965).
(11) R. F. Stewart, E. R. Davidson, and W. T. Simpson, *J. Chem. Phys.*, **42**, 3175 (1965).
(12) D. T. Cromer, *Acta Crystallogr.*, **18**, 17 (1965).
(13) W. C. Hamilton, *Acta Crystallogr.*, **18**, 502 (1965).
(14) See paragraph at end of paper regarding supplementary material.
(15) D. P. Freyberg, G. M. Mockler, and E. Sinn, *J. Chem. Soc., Dalton Trans.*, in press.
(16) E. J. Cukauskas, B. S. Deaver, Jr., and E. Sinn, *J. Chem. Soc., Chem. Commun.*, 698 (1974); E. J. Cukauskas, B. S. Deaver, Jr., and E. Sinn, to be submitted for publication.
(17) R. J. Butcher and E. Sinn, submitted for publication.
(18) R. J. Butcher, J. R. Ferraro, and E. Sinn, unpublished results.